

Fig. 3. (a) Space-time diagram where plot sequentially describes A, B, C, (on voyage), B, C, (on return), etc. (b) Diagram where A and B discuss a voyage recently completed by C and then converse about the similar part of a trip previously made by B. Dash-dash lines in (b) represent flashbacks. (c) Diagram where C has promised to sell some land (shading stands for promise) to B; the promise stands unaffected by a "crossing of the ways", during extended discussions with A, and for part of the return journey; repeated reflections on a part of the conversation lead to correspondence, however, which ultimately secures B's release from the promise, A's agreement to purchase, and C's death from the strain at an intermediate point.

LITERATURE CITED

- Gamow, George. 1962. *One, Two, Three . . . Infinity*. Bantam Books, New York.
- Eaton, Jeanette. 1944. *Lone Journey*. Harcourt, Brace & Co., New York.
- Stewart, George. 1947. *Storm*. Modern Library, New York.
- Mandl, F. 1959. *Introduction to Quantum Field Theory*. Interscience Publishers, New York.

JOURNAL OF THE TENNESSEE ACADEMY OF SCIENCE

Volume 43, Number 3, July, 1968

ANALOG MODEL FOR PLATES WITH IN-PLANE EDGE LOADING

GEORGE R. BUCHANAN

AND

THOMAS W. HUDNALL

*Tennessee Technological University,
Cookeville, Tennessee 38501 and
Tennessee Eastman Company,
Kingsport, Tennessee 37660*

ABSTRACT

Finite difference equations for plates with in-plane edge loadings are derived from an analog model of the plate. The critical buckling load is obtained for a square plate with two interior stiffeners to illustrate the use of the model. The effects of both the flexural rigidity and torsional rigidity are included in the analysis.

INTRODUCTION

In recent years there has been increased research in analyzing plates using finite difference techniques. Considerable progress has been made using finite difference techniques combined with an analog model of a plate. The advantage of the analog model becomes apparent when difficult boundary conditions and discontinuities are encountered for the plate.

The analog model used in this paper is an extension of the model first suggested by N. M. Newmark.¹

The plate analog has been used extensively by other investigators. In particular, the work of A.H.-S. Ang and W. S. Prescott^{2,3} will be referred to repeatedly in this paper. Ang and Prescott have extended the work of Newmark to include the effect of transverse stiffeners in a deflection analysis. In this study, the application of Newmark's plate analog has been extended to include the effect of in-plane edge loadings. The analog model was then used to derive equations for determining the stresses, deflections or critical buckling loads for the plate. Ang and Prescott's plate model has been used to evaluate the effect of plate stiffeners on the critical buckling load.

Notation: The terms adopted for use in this paper are defined where they first appear in the text and are listed alphabetically.

DERIVATION OF EQUATIONS

The differential equation which expresses the deflection of plates in terms of lateral and in-plane loading has been derived by Timoshenko and Gere⁴ as

$$w_{,xxxx} + 2w_{,xxyy} + w_{,yyyy} = (q + N_x w_{,xy} + N_y w_{,yy} + 2N_{xy} w_{,xy})/D \quad (1)$$

where a comma followed by a variable represents partial differentiation; also, w is the deflection, q is the lateral load per unit area, N_x and N_y are the in-plane forces in the x and y directions respectively, N_{xy} is the in-plane shear force and D is defined as follows

$$D = \frac{Et^3}{12(1-\nu^2)} \quad (2)$$

where E is Young's Modulus, t is the thickness and ν is poisson's ratio.

The finite difference equivalent of Eq. (1) can be obtained using the plate analog shown in Fig. 1. The plate has been represented by a physical model composed of a network of rigid beams connected at the grid points by elastic hinges. The parallel beams are connected by torsional springs to represent the twisting moments and linear springs to represent the in-plane shearing forces. The physical model is assumed to have the following characteristics;

- (1) The beams are weightless and rigid.
- (2) The traverse external loads are concentrated at the elastic hinges.
- (3) The resultants of direct stresses are bending moments acting at the elastic hinges and at the ends of each beam.
- (4) The resultants of the vertical stress are shearing forces acting at the elastic hinges and at the end of each beam.
- (5) The resultants of the horizontal shearing stresses are twisting moments concentrated in the torison springs.
- (6) The resultant in-plane stresses are horizontal forces acting at the elastic hinges and at the end of each bar.
- (7) The resultants of the in-plane shearing stresses are in-plane forces concentrated in the linear springs.

Interior point

Figure 2 shows the forces and moments acting on a typical interior elastic hinge and adjacent rigid beams. The finite difference operator will be derived by first summing the vertical forces acting on joint "O" as follows

$$V_{oe} - V_{ow} - V_{os} + V_{on} + Q = 0 \quad (3)$$

Equation (3) may be expressed in terms of moments and in-plane forces by summing moments about the end of each beam which connects to joint "O" and substitut-

ing into Eq. (3). For example, summing the moments about end "e" of beam oe yields

$$hV_{oe} = M_{ex} - M_{ox} + M_{xy}^A - M_{xy}^B + hN_{oe} \frac{dw}{dx} \Big|_{oe} - \frac{h}{2} N_{xy}^B \frac{dw}{dy} \Big|_B - \frac{h}{2} N_{xy}^A \frac{dw}{dy} \Big|_A \quad (4)$$

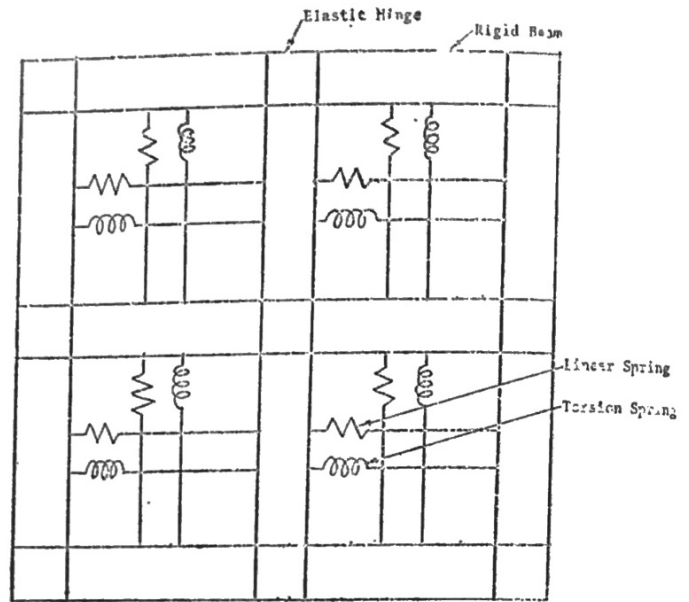


Figure 1. Plate Analog

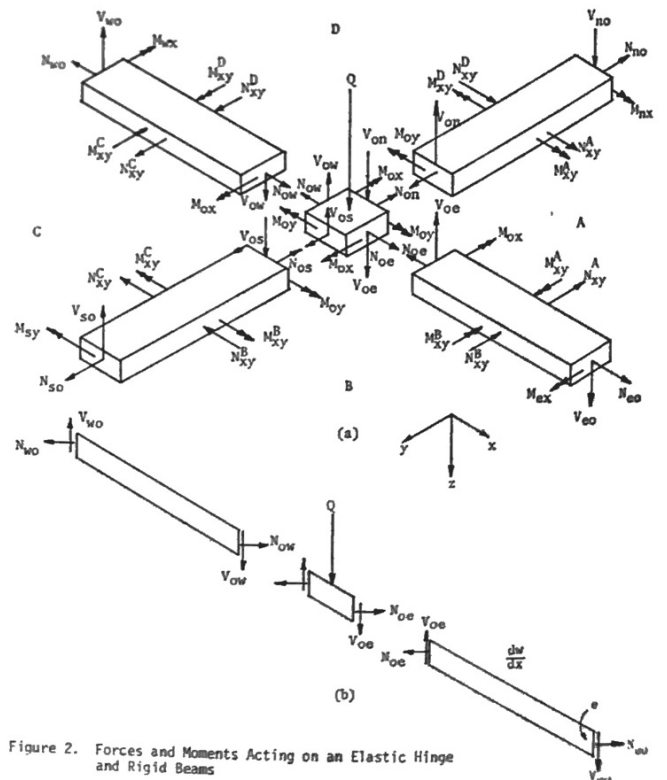


Figure 2. Forces and Moments Acting on an Elastic Hinge and Rigid Beams

where M and N represent the total moments and in-plane forces acting across a grid width and are as shown in Fig. 2, h is the length of the beam and $\frac{dw}{dx} \Big|_{oe}$ indicates the slope to be evaluated along beam oe. In writing Eq. (4) it has been assumed that the slope is small, i.e. $\sin \frac{dw}{dx} \approx \frac{dw}{dx}$. Substituting moment equations into Eq. (3) and assuming that $N_{oe} =$

Now $N_x = N_x, N_{on} = N_{os} = N_y$ and $N_{xy} = N_{xy}$
 $N_{xy} = N_{xy} = N_{xy}$ the following equation results.

$$M_{ex} - 2M_{ox} + M_{wx} + M_{ny} - 2M_{oy} + M_{sy} + 2(M_{xy}^A - M_{xy}^B + M_{xy}^C - M_{xy}^D) =$$

$$- [Q + hN_x \left(\frac{dw}{dx} \Big|_{oe} - \frac{dw}{dx} \Big|_{ow} \right) + hN_y \left(\frac{dw}{dy} \Big|_{os} - \frac{dw}{dy} \Big|_{on} \right)]$$

$$+ \frac{h}{2} N_{xy} \left(\frac{dw}{dx} \Big|_A - \frac{dw}{dy} \Big|_B - \frac{dw}{dx} \Big|_C + \frac{dw}{dy} \Big|_D + \frac{dw}{dx} \Big|_E + \frac{dw}{dy} \Big|_F \right)$$

Equation (5) may be written entirely in terms of deflections by substituting the appropriate finite difference approximations for the moments and slopes. For the typical joint "0" a few examples are as follows:

$$M_{ox} = - \frac{D}{h^2} [W_w - 2W_0 + W_e + (W_n - 2W_0 + W_s)]$$

$$\frac{dw}{dx} \Big|_{oe} = \frac{W_e - W_0}{h}; \quad \frac{dw}{dy} \Big|_{on} = \frac{W_0 - W_n}{h}$$

For a typical panel area "A"

$$M_{xy}^A = \frac{D}{h^2} [W_n - W_{ne} + W_e - W_c - (W_n - W_{ne} + W_e - W_0)]$$

$$\frac{dw}{dx} \Big|_A = \frac{1}{h} \left(\frac{W_{ne} + W_e}{2} - \frac{W_n + W_0}{2} \right)$$

$$\frac{dw}{dy} \Big|_A = \frac{1}{h} \left(\frac{W_0 + W_e}{2} - \frac{W_n + W_{ne}}{2} \right)$$

The left hand side of Eq. (5) may be represented by the familiar fourth order finite difference operator⁵ while the right hand side reduces to the following:

$$Q + N_x \begin{bmatrix} & & & \\ & & -2 & \\ & & & \\ & & & \end{bmatrix} + N_y \begin{bmatrix} & & & \\ & & & \\ & & -2 & \\ & & & \end{bmatrix} + 2N_{xy} \begin{bmatrix} & & & \\ & & & \\ & & & \\ & & & \end{bmatrix} w \quad Op. (1)$$

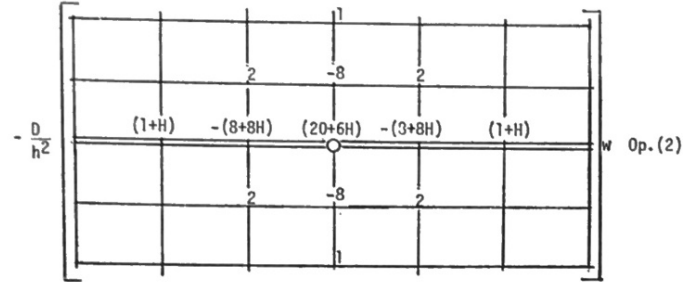
Operator (1) when used with the bi-Laplacian operator yields the equivalent finite difference expression for Eq. (1).

In what follows the operators obtained by summing bending and twisting moments will be referred to as M-operators and the operators derived from the in-plane forces will be referred to as N-operators. For the

remaining derivations it will be assumed that N_{xy} is zero.

Operators for Stiffened Plates

The M-operator for a point on an interior stiffener was derived by Ang and Prescott⁸ as



where H is a measure of the flexural stiffness of the plate stiffener, defined as

$$H = EI/Dh \quad (8)$$

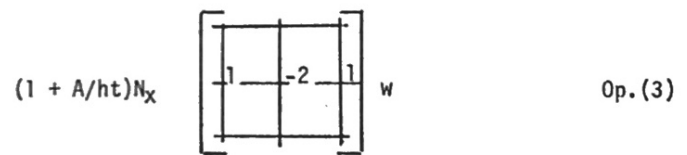
The N operator must be derived in terms of the ratio of the in-plane force acting on a stiffened grid to the in-plane force acting on an unstiffened grid as follows:

$$P/N = (ht + A)/ht \quad (9)$$

where h . t is the area of the plate along a finite difference grid, A is the area of the stiffener and P is the in-plane force acting on a stiffened grid. From Eq. (9),

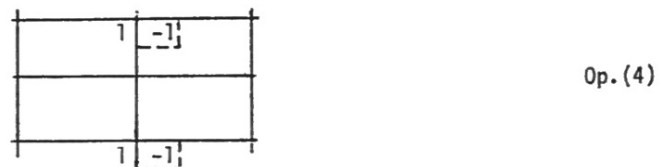
$$P = (1 + A/ht) N \quad (10)$$

hence, the N_x - operator for a point on an interior stiffener is



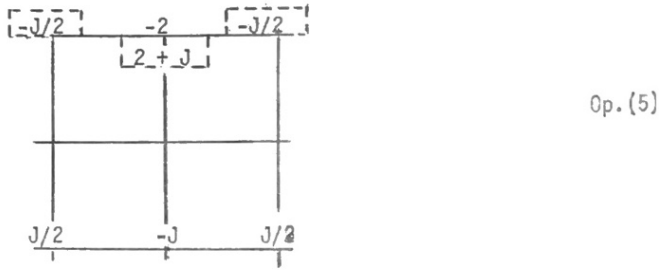
Operators Related to Fictitious Points

Operators relating fictitious points due to the presence of stiffeners to other points on the plate have been derived previously^{2,3} and will be included for the sake of completeness. The torsional stiffness of the stiffener will create a discontinuity at the junction between the plate and stiffener. The operator can be developed from the curvature expression as



where the numbers inside the boxes refer to the fictitious points required for equilibrium.

Equilibrium of moments about an axis of the beam yields an additional operator



Op. (5)

where J is a measure of torsional stiffness of the stiffener defined as

$$J = \frac{GC}{Dh}$$

APPLICATION

Analysis for Critical Buckling Load

To illustrate the use of the operators which have been presented the critical buckling load will be calculated for a square plate with two longitudinal stiffeners. The plate to be analyzed is shown in Fig. 3. Writing a finite difference equation at each grid point on the plate will result in a matrix equation representing the coefficients of the finite difference equations and the unknown deflections as follows:

$$[S] [w] = (N_x [A] [w] + N_y [B] [w] + N_{xy} [C] [w]) \frac{h^2}{d} \quad (11)$$

where $[S]$, $[A]$, $[B]$, and $[C]$ are the coefficient matrices and h is the finite difference grid spacing.

For this illustrative example it will be assumed that N_{xy} is zero, and that N_y is either zero, one half of N_x are equal to N_x , hence Eq. (11) may be written as

$$[S] [w] = N_x \left[[A] + \alpha[B] \right] [w] \frac{h^2}{D}$$

or

$$[S] [w] = N_x [D] [w] \frac{h^2}{D} \quad (12)$$

The solution of Eq. (12) to obtain the critical buckling load has been discussed previously; for instance, Salvadori⁶ has illustrated a technique for analysis with a discussion of the error involved. Kapur and Hartz⁷ have discussed the solution of Eq. (12) in conjunction with a finite element analysis for the buckling problem. For the example problem to be presented, the presence of the fictitious points in the plate will develop finite difference equations in which zeros will appear along the diagonal of matrix $[D]$. Additional matrix operations⁸ will be required to reduce the matrix equation to the standard form.

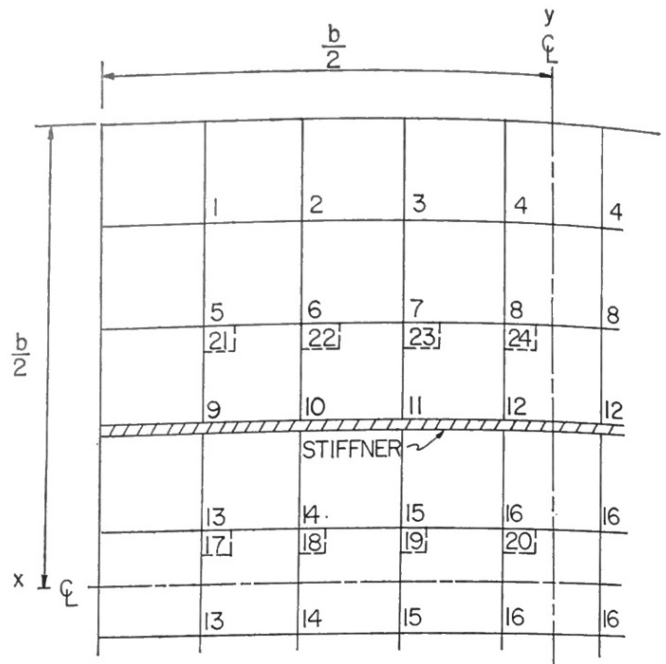


Figure 3. Finite Difference Grid for a Square Plate with Two Stiffeners

A 24×24 matrix results when an equation is written for each grid point of Fig. 3. The points inside the dashed boxes are fictitious and the $[D]$ matrix of Eq. (12) will have zero elements along the diagonal for elements corresponding to points 17 through 24. Operator (4) was used for points 17 through 20 and Op. (5) for points 21 through 24. Equation (12) should be partitioned as follows

$$\begin{bmatrix} S_{11} & \dots & S_{16} & \dots & S_{124} \\ \vdots & & \vdots & & \vdots \\ \vdots & & S_{16} & \dots & \vdots \\ \vdots & & \vdots & & \vdots \\ S_{24} & \dots & S_{24} & \dots & S_{24} \end{bmatrix} \begin{bmatrix} w_1 \\ \vdots \\ w_{16} \\ \vdots \\ w_{24} \end{bmatrix} = \frac{h^2 N_x}{D} \begin{bmatrix} D_{11} & \dots & D_{10} & \dots & \dots \\ \vdots & & \vdots & & \vdots \\ \vdots & & D_{16} & \dots & \vdots \\ \vdots & & \vdots & & \vdots \\ \vdots & & \vdots & & 0 \\ \vdots & & \vdots & & \vdots \\ \vdots & & \vdots & & \vdots \\ \vdots & & \vdots & & 0 \end{bmatrix} \begin{bmatrix} w_1 \\ \vdots \\ w_{16} \\ \vdots \\ w_{24} \end{bmatrix} \quad (13)$$

Both matrices have been partitioned along the row and column which corresponds to the first zero diagonal element in $[D]$. Rewriting Eq. (13) yields

$$\begin{bmatrix} S_{IV} & S_{II} \\ \vdots & \vdots \\ S_{III} & S_I \end{bmatrix} \begin{bmatrix} W \\ \vdots \\ W \end{bmatrix} = \frac{h^2 N_x}{D} \begin{bmatrix} D & \vdots \\ \vdots & \vdots \\ \vdots & 0 \end{bmatrix} \begin{bmatrix} W \\ \vdots \\ W \end{bmatrix} \quad (14)$$

The original 24×24 matrix may be reduced to a 16×16 matrix corresponding to the equations for the real grid points which lie on the plate. The resulting matrix equation is

$$\left[[S_{IV}] - [S_{II}] [S_I]^{-1} [S_{III}] \right] [w] = \frac{h^2}{D} N_x [D] [w] \quad (15)$$

In order to obtain the lowest eigenvalue for Eq. (15) using matrix iteration it will be necessary to multiply by the inverse of the matrix on the left hand side and divide by N_x .

Critical buckling loads were obtained for various combinations of H, J and stiffener area. The results are shown in Tables I, II and III as the value of K to be substituted in the following equation:

$$(N_x)_{cr} = \frac{K \pi^2 D}{b^2} \quad (16)$$

The most important result of this study is the evaluation of the effect of the torsional rigidity on the critical

buckling load. As can be seen from Tables I, II and III the effect of increasing the torsional rigidity is to decrease the critical buckling load.

Table IV shows the effect of including the torsional rigidity of the stiffener when the in-plane loading is normal to the stiffener. When only N_y is considered the critical load decreases as the torsional rigidity increases.

TABLE I
CRITICAL BUCKLING LOADS FOR A PLATE WITH TWO STIFFENERS AND $N_y = 0$.
VALUES OF K TO BE USED IN EQUATION 16

EI/bD	2.5			5.0			7.5			10.0			
	A/bt	.01	.05	.1	.01	.05	.1	.01	.05	.1	.01	.05	.1
JC/bD = 0		10.88	9.79	8.69	17.57	15.89	14.17	23.93	21.73	19.46	29.96	27.33	24.58
1		9.45	8.51	7.56	16.13	14.59	13.01	22.48	20.42	18.30	28.51	26.02	23.40
	2	9.18	8.26	7.34	15.87	14.35	12.80	22.22	20.18	18.09	28.26	25.78	23.19

TABLE II
CRITICAL BUCKLING LOAD FOR A PLATE WITH TWO STIFFENERS AND $N_y = .5N_x$.
VALUES OF K TO BE USED IN EQUATION 16

EI/bD	2.5			5.0			7.5			10.0			
	A/bt	.01	.05	.1	.01	.05	.1	.01	.05	.1	.01	.05	.1
JC/bD = 0		7.30	6.80	6.26	11.67	10.93	10.11	15.61	14.72	13.71	17.15	16.95	*
1		6.45	5.99	5.51	10.99	10.25	9.45	15.35	14.34	13.25	*	***	17.10
	2	6.30	5.85	5.38	10.89	10.16	9.36	15.33	14.30	13.21	*	18.88	17.09

TABLE III
CRITICAL BUCKLING LOAD FOR A PLATE WITH TWO STIFFENERS AND $N_y = N_x$.
VALUES OF K TO BE USED IN EQUATION 16

EI/bD	2.5			5.0			7.5			10.0			
	A/bt	.01	.05	.1	.01	.05	.1	.01	.05	.1	.01	.05	.1
JC/bD = 0		5.49	5.20	4.88	8.71	8.30	7.83	9.67	9.58	9.48	10.00	9.84	9.87
1		4.91	4.64	4.34	8.52	8.03	7.51	*	*	*	*	*	*
	2	4.82	4.55	4.26	8.51	8.01	7.48	*	*	*	*	*	*

TABLE IV
CRITICAL BUCKLING LOAD FOR A PLATE WITH TWO STIFFENERS AND $N_x = 0$.
VALUES OF K TO BE USED IN EQUATION 16

EI/bD	5	2.5	1	.5	.25
JC — = 0 bD	** 11.36	** 10.45	6.89	5.43	4.70
1	—	—	6.51	5.05	4.31
2	—	—	6.31	4.82	4.07

DISCUSSION

The effect of increasing the torsional rigidity of the plate stiffeners resulted in a decrease in the critical load for all loading combinations investigated in this study. The values of K in the Tables which have been marked with an asterisk (*) were not obtained. The matrix iteration technique did not converge in a reasonable amount of time using an IBM 1710 computer system. The quantities marked with a double asterisk (**) correspond to a mode shape in which the stiffener did not buckle. The plate deflected upward between the stiffeners and downward on the outside of the stiffeners. The mode shape for the K value marked with a triple asterisk (***) indicated upward deflection for points 3 and 4 (See Fig. 3) and downward deflection for all other grid points.

Numerous buckling problems were solved during the investigation. In general, the accuracy of an eigenvalue solution was not as good as that of the deflection solution for the same grid spacing.

The analog model has been used to study the effects of stiffeners on the buckling of plates with cut-outs^o. The results of that study will be published as soon as experimental verification can be obtained.

CONCLUSIONS

It has been shown that a physical model of a plate structure can be used to advantage for deriving finite difference equations when discontinuities or difficult boundary conditions are encountered. The solution of plate buckling problems using finite differences approximations has been illustrated. A matrix manipulation technique for substituting the boundary condition equations or fictitious point equations into the plate equations has been presented.

It has been shown that the effect of the torsional rigidity of the stiffener on the critical load is small. However, increasing the torsional rigidity tends to decrease the critical buckling load.

ACKNOWLEDGEMENTS

The authors are indebted to the Tennessee Technological University for supporting this research work through a faculty research grant and through the facilities of the D. W. Mattson Computer Center.

NOTATION

A	— Area of stiffener
b	— Length of square plate
C	— Torsion constant
D	— See Eq. (2)
E	— Young's Modulus
G	— Shear Modulus
h	— Grid spacing
H	— EI/Dh
I	— Moment of inertia
J	— GC/Dh
K	— See Eq. (16)
M_x, M_y, M_{xy}	— Bending and twisting moments
N_x, N_y, N_{xy}	— In-plane edge loading
P	— In-plane force acting on a stiffened grid
q	— Lateral load per unit area
Q	— Total lateral load at an elastic hinge
t	— Plate thickness
V	— Shear
w	— Deflection
x, y	— Coordinates
α	— Ratio of N_y to N_x
ν	— Poisson's ratio
[S], [A], [B], [C], [D]	— Finite difference coefficient matrices

LITERATURE CITED

1. "Numerical Methods of Analysis of Bars, Plates, and Elastic Bodies", by N. M. Newmark, Chap. 9, Numerical Methods of Analysis in Engineering, ed. by L. E. Grinter, New York, MacMillan, 1949.
2. "Equations for Plate-Beam Systems in Transverse Bending," A.H.-S. Ang and W. S. Prescott, Proc., ASCE, Vol. 87, No. EM6, 1961, pp. 1-15.
3. "Analysis of Clamped Square Plates Containing Openings with Stiffened Edges", by W. S. Prescott, Ph.D. Thesis, University of Illinois, Urbana, Ill., 1962.
4. "Theory of Elastic Stability", by S. P. Timoshenko and J. M. Gere, New York, McGraw Hill, 1961, Chap. 8.
5. "Theory of Plates and Shells", by S. P. Timoshenko and S. Woinowsky-Krieger, New York, McGraw Hill, 2nd ed., 1959, Chap. 10.
6. "Numerical Computation of Buckling Loads by Finite Differences", by M. G. Salvadori, Trans., ASCE, Vol. 116, 1951, pp. 590-636.
7. "Stability of Plates Using the Finite Element Method", by K. K. Kapur and B. J. Hartz, Proc., ASCE, Journal of the Engineering Mechanics Division, Vol. 92, No. EM2, Ap. 1966, pp. 177-195.
8. "Application of a General Finite Difference Method for Calculating Bending Deflections of Solid Plates", by W. C. Walton, NASA TND-536, 1960.
9. "Analog for Plates with In-Plane Edge Loading", by T. W. Hudnall, M.S. Thesis, Tennessee Technological University, Cookeville, Tennessee, Aug. 1967.